

## Research Paper

DESIGN OF A LOW-VOLTAGE LOW-DROPOUT  
REGULATORS R Patil<sup>1\*</sup> and Naseeruddin<sup>1</sup>\*Corresponding Author: S R Patil, ✉ [sadanandpatil001@gmail.com](mailto:sadanandpatil001@gmail.com)

A low-voltage Low-Dropout (LDO) regulator that converts an input of 1 V to an output of 0.85-0.5 V, with 90-nm CMOS technology is proposed. A simple symmetric operational transconductance amplifier is used as the Error Amplifier (EA), with a current splitting technique adopted to boost the gain. This also enhances the closed-loop bandwidth of the LDO regulator. In the rail-to-rail output stage of the EA, a power noise cancellation mechanism is formed, minimizing the size of the power MOS transistor. Furthermore, a fast responding transient accelerator is designed through the reuse of parts of the EA. These advantages allow the proposed LDO regulator to operate over a wide range of operating conditions while achieving 99.94% current efficiency, a 28-mV output variation for a 0-100 mA load transient, and a power supply rejection of roughly 50 dB over 0-100 kHz. The area of the proposed LDO regulator is only 0.0041 mm<sup>2</sup>, because of the compact architecture.

Keywords: Fast transient response, High power supply rejection, Low-Dropout (LDO) regulator, Low-voltage, Small area

## INTRODUCTION

POWER management unit with several integrated regulators is widely used in modern battery powered portable devices. These power management schemes often use a primary switching regulator and several postregulators (Lee *et al.*, 2010; and El-Nozahi *et al.*, 2010). The primary switching regulator converts the high dc voltage level of the battery (e.g., 4.2-2.7 V) into a low dc voltage level (e.g., 1 V) with a high conversion

efficiency (>90%). The postregulators also generate several independent power sources for multiple voltage domains. The switching regulator inevitably generates voltage ripples over the range of the switching frequency. The switching frequency of the regulator often lies within a low-frequency band of a few 10-100 kHz to reduce switching power loss. The post-regulators should, therefore, be able to provide a good Power Supply Rejection (PSR) ability to suppress these unwanted low-frequency

<sup>1</sup> Department of ECE, BITM, Bellary, Karnataka, India.

noises. To further maintain high power efficiency, minimize the impact on target load circuits, and reduce cost, these post regulators must operate at low voltage and low quiescent current ( $I_Q$ ), achieve a fast transient response with a small out-put variation, and minimize their area. The low-dropout (LDO) regulator has a simple architecture and a fast-responding loop, which makes it the best candidate to implement these post regulators.

A number of previous papers focused on enhancing the transient response (Hazucha *et al.*, 2005; Al-Shyoukh *et al.*, 2007; Lam and Ki, 2008; Lin *et al.*, 2008; Garimella *et al.*, 2010; Chen *et al.*, 2011; Hu *et al.*, 2011; and Zhan and Ki, 2011) or the PSR (Al-Shyoukh *et al.*, 2007; Lam and Ki, 2008; El-Nozahi *et al.*, 2010; Patel and Rincon-Mora, 2010; and Zhan and Ki, 2010) or both of LDO regulators. The designs in (Hazucha *et al.*, 2005; Al-Shyoukh *et al.*, 2007; Lam and Ki, 2008; and Chen *et al.*, 2011) use either a large driving current or additional circuits, which consume a significant  $I_Q$ . The design in (Lin *et al.*, 2008) consumes a small  $I_Q$ , yet has a large output variation during the load transient. Further, a complex compensation circuit (Lin *et al.*, 2008) or a high-gain cascode Error Amplifier (EA) (Garimella *et al.*, 2010) complicates the LDO regulator design and is not feasible for low-voltage systems ( $\leq 1$  V) that are using advanced technology. All the previous regulators are unable to achieve sub 1-V operation.

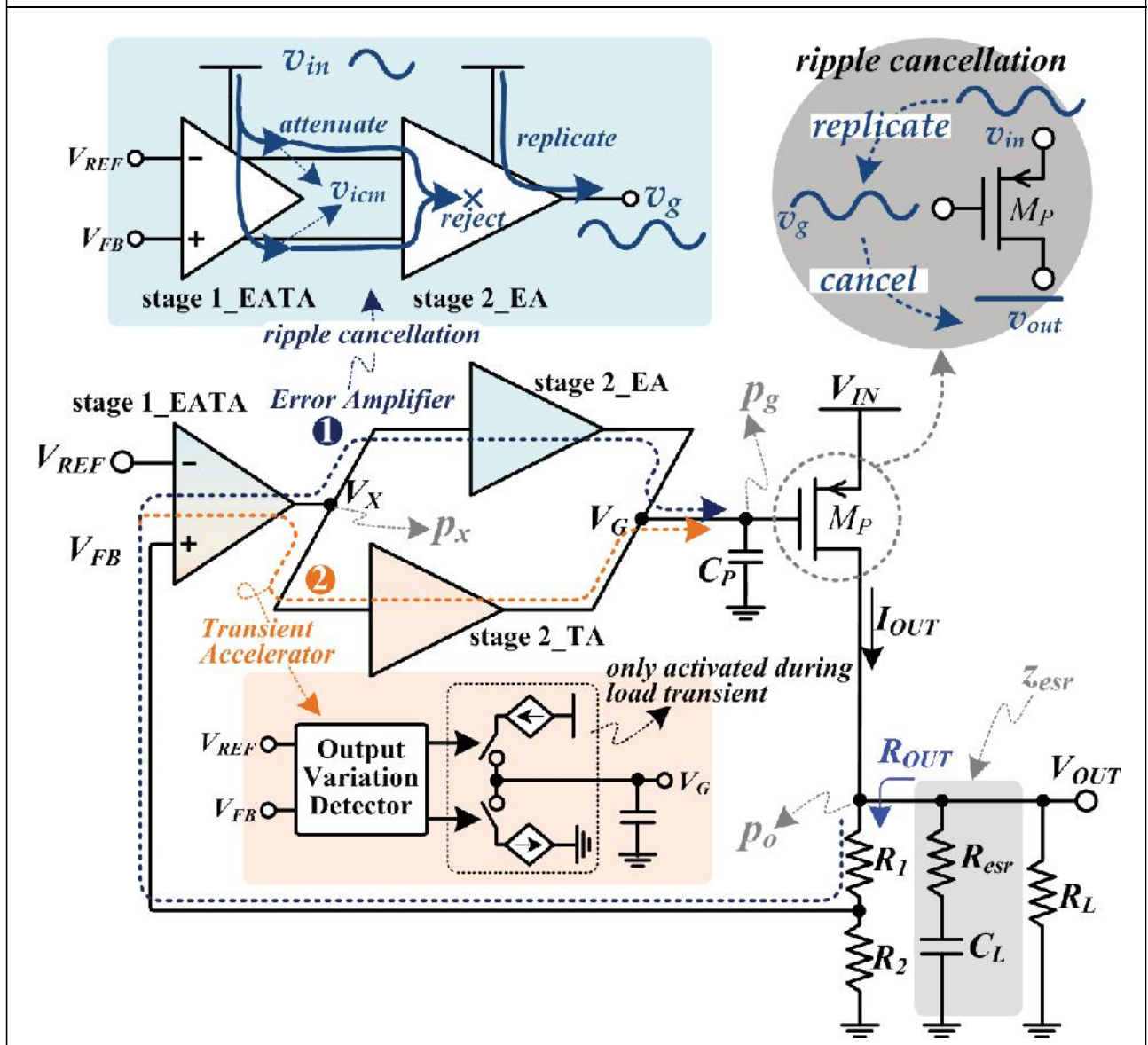
## DESIGN CHALLENGES AND CONCEPTS OF THE PROPOSED LOW-VOLTAGE LDO REGULATOR

A basic LDO regulator is mainly composed of a biasing circuit, an EA, a power MOS transistor ( $M_p$ ), and a feedback network, as shown in Figure 1. Now, the Transient Accelerator (TA) is removed. An off-chip output capacitor ( $C_L$ ) is used to mitigate the output variations during the load transient. The design challenges and concepts in designing a low-voltage LDO regulator are summarized briefly in the following sections.

### Low Supply (Input) Voltage and Low $I_Q$

A high loop gain is mandatory in LDO regulator design to achieve optimum performance values such as accurate output (line/load regulation) and PSR. A low supply voltage and output-resistance reduction induced by a shrinking technology limit the achievable gain of the EA. Thus, there are many auxiliary circuits that consume considerable  $I_Q$  that are proposed to enhance performance. A  $M_p$  with a significant size is required for a specific load current when an LDO regulator sinks current from a low voltage power source. Thus, the EA requires a higher current slew rate to drive the  $M_p$ . To achieve low-voltage operation, an EA with not more than three stacked transistors between the supply voltage and ground is preferred. Each of the transistors, therefore, has more voltage space to stay in the saturation region. A possible candidate can be as simple as an Operational Transconductance Amplifier (OTA) with a low-cost gain-boosting technique like current splitting (Sansen, 2008). The EA also requires a wide output swing to minimize the size of the  $M_p$ , and hence relieve the requirement on output current slew rate of the EA.

Figure 1: Conceptual Block Diagram of the Proposed LDO Regulator



### Fast Transient Response

The transient response, includes the voltage variation (spike) and recovery (settling) time during the load current transient. The voltage variation is more important than the recovery time, as even a small output-voltage variation (e.g., 50 mV) can cause severe performance degradation to the load circuit operating at an ultralow supply voltage (e.g., 0.5 V). To reduce the output-voltage variation, both a

large closed-loop bandwidth of the LDO regulator and a large output current slew rate of the EA are required (Rincon-Mora, 2009). Increasing the closed-loop bandwidth may, however, affect the pole/zero locations and the circuitry may become too complex, consuming more  $I_o$  (Al-Shyoukh *et al.*, 2007; and Chen *et al.*, 2011). The concept of the TA, shown in Figure 1, is, therefore, adopted to conditionally provide extra charging/discharging current

paths (slew current), depending on the status of the output variation detector.

### Power Supply Rejection

To provide a clean and accurate output voltage with a low voltage level ( $\leq 1$  V), noise suppression is paramount. An  $n$ -type power MOS transistor or a cascoded power MOS transistor structure can achieve a high PSR; however, they are unfeasible for sub 1-V operations. As an LDO regulator adopts a  $p$ -type power MOS transistor, either a high loop gain or good noise cancellation at node  $V_G$  can achieve a high PSR. It is, however, difficult to achieve a high loop gain with a low supply voltage. In addition, the circuit for the power noise cancellation mechanism increases the design complexity and consumes extra  $I_Q$ . The concept of resources sharing power noise cancellation mechanism as shown in Figure 1 is thus proposed. The first stage (stage 1\_EATA) of the EA attenuates the power noise, whereas the second stage (stage 2\_EA) of the EA rejects the common mode noise ( $v_{icm}$ ) at its inputs, and creates a replica of the supply noise at the output. The stage 1\_EATA is shared by the EA and TA, saving the cost and  $I_Q$ .

### Small Area

In a low-voltage LDO regulator design, several performance enhancing auxiliary circuits and a large  $M_p$  occupy consider-able space. A wide output swing EA can reduce the size of the  $M_p$ . To support a wide load current range (e.g., 0-100 mA) and a wide output-voltage range (e.g., 0.5-0.85 V), the  $M_p$  may enter the triode region when under a heavy load condition (large  $V_{SG}$ ) with a low-dropout voltage (small  $V_{SD}$ ). The  $M_p$  should, therefore, be large

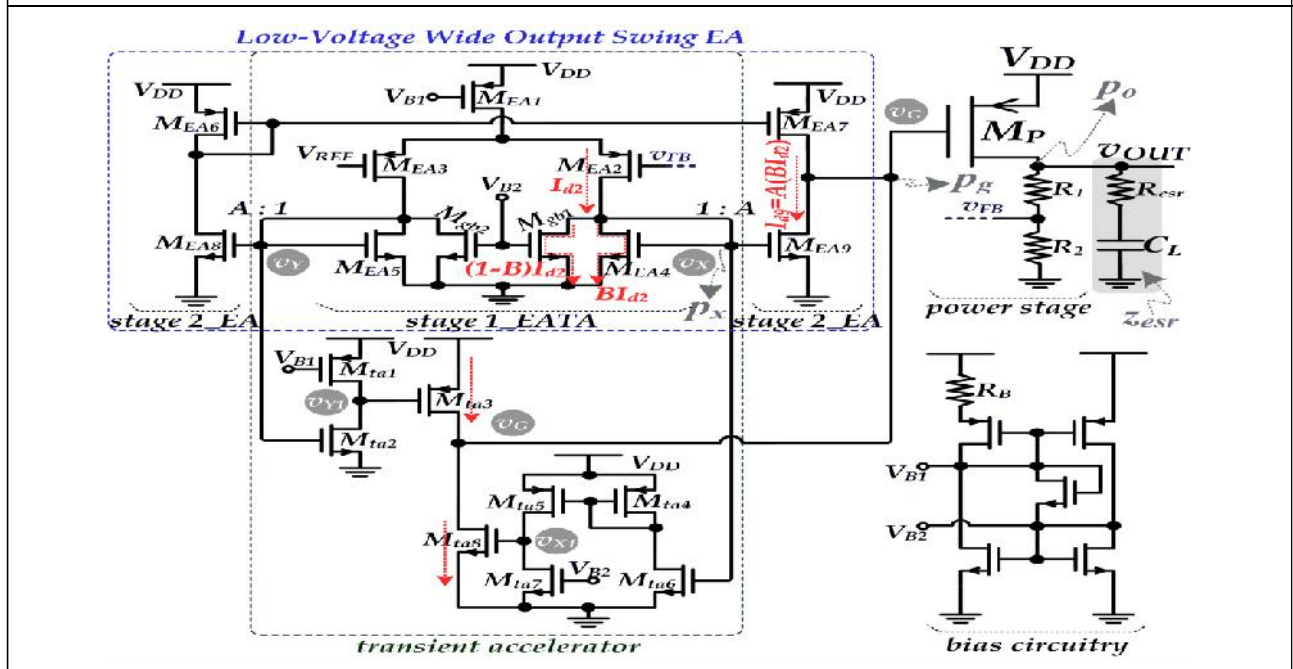
enough to make the intrinsic gain of the  $M_p$  close to one at the triode region and maintain a high loop gain in the LDO regulator. Similarly, the LDO regulator can respond to the load current transient in time for such a wide range of operating conditions.

## CIRCUIT REALIZATION AND SIMULATION RESULTS

To achieve the required goals of compact and low-voltage operation while achieving a fast transient response, low  $I_Q$  and high PSR, four aspects of the proposed LDO regulator are optimized. The circuit schematic is shown in Figure 2. We first apply the simple symmetric OTA as the EA, composed of  $M_{EA1}$ - $M_{EA9}$ , where  $gm_{\bar{ii}} = 1-9$ ,  $rO_{\bar{ii}} = 1-9$ , and  $\lambda_{\bar{ii}} = 1-9$  represent the corresponding transconductance, output resistance, and the channel length modulation coefficients, respectively. The OTA-type EA requires no compensation capacitor, and operates at a minimum supply voltage ( $V_{DD, \min}$ ) equal to one threshold voltage plus twice the overdrive voltage ( $V_{DD, \min} = V_T + 2 \times V_{OV}$ ). Thus, the EA can operate with a low supply voltage ( $\leq 1$  V). The symmetric structure of the EA also has a low input offset voltage for the regulator to achieve an accurate output. Furthermore, the impedances at node  $v_x$  and  $v_y$  are low enough to push the nondominant pole ( $p_x$ ) to a sufficient high frequency so as not to affect the system stability.

The EA achieves a rail-to-rail output swing at node  $V_G$  by the output stage ( $M_{EA7}$  and  $M_{EA9}$ ); therefore, the size of the  $M_p$  can be minimized for a specific load current requirement. Reducing the size of the  $M_p$  significantly reduces the circuit area and contributes to a smaller gate capacitance. This allows the EA

Figure 2: Circuit Schematic of the Proposed LDO Regulator



to drive the  $M_p$  by a large enough slew rate with a relatively low biasing current. The gain of the EA ( $A_{EA0}$ ) is as follows:

$$\begin{aligned}
 A_{EA0} &= gm \times A \times (rO7 || rO9) \\
 &\approx gm2 \times A \times rO9 \\
 &= \frac{2I_{d2}}{V_{oV2}} \times Ax \frac{1}{9 \times Ax I_{d2}} \\
 &= \frac{2}{V_{o2} \times 9} \dots(1)
 \end{aligned}$$

where we assume  $(rO7 \_ rO9)$  and let  $\{I_{d2}, V_{oV2}, A\}$  represent the bias current, overdrive voltage of  $M_{EA2}$ , and current ratio between the first and second stages of the EA, respectively. The  $A_{EA0}$  in (1) is too low to achieve a fast transient response and high PSR. Therefore, we apply the current splitting technique to boost the gain by maintaining  $gm2$  and increasing  $rO9$ . The transistors  $M_{gb1}$  and  $M_{gb2}$  can reduce the bias current being mirrored to the second stage of the EA. Thus,

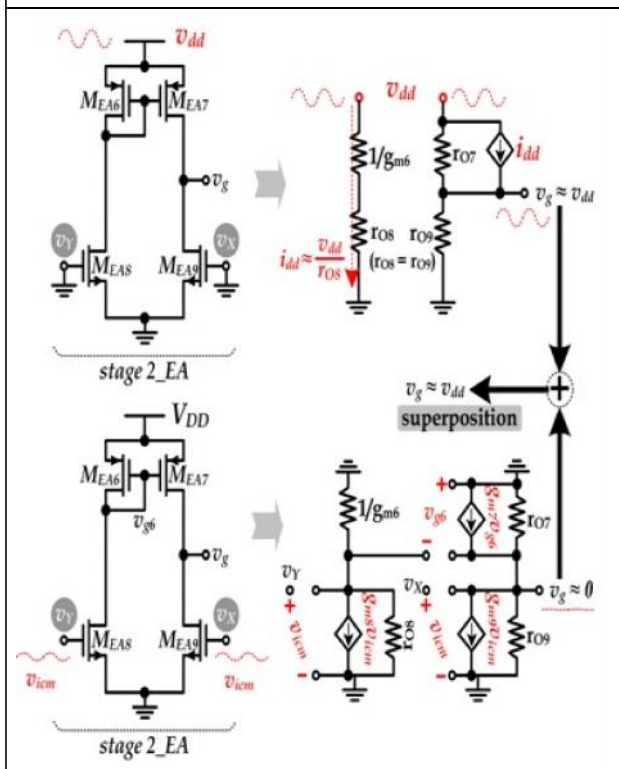
the gain of the modified EA ( $A_{EAM}$ ) is boosted by a factor of  $1/B$  as follows:

$$\begin{aligned}
 A_{EAM} &\approx gm2 \times A \times rO9 \\
 &= \frac{2I_{d2}}{V_{o2}} \times Ax \frac{1}{9 \times Ax B \times I_{d2}} \\
 &= \frac{A_{EA0}}{B} \dots(2)
 \end{aligned}$$

where  $B$  is the current splitting ratio and is  $<1$ .

A  $p$ -type device is chosen to construct the power MOS transistor  $M_P$ , because of the low supply voltage and low-dropout voltage requirements. The gain-boosted OTA-based EA improves the loop gain of the LDO regulator, which in turn enhances the PSR performance. In addition, we create a replica of the power noise at the gate terminal of the  $M_p$  to cancel out the power noise at the source terminal of  $M_p$ . This further improves the PSR performance. To reduce the area and  $I_Q$ , we use the existing EA to replicate the power

Figure 3: Low-Frequency, Small-Signal Model of the EA Output Stage (Stage 2\_EA) for Ripple Cancellation Analysis



noise instead of using an auxiliary circuit. The two equivalent resistors between the output nodes ( $v_x$  and  $v_y$ ) of the first stage of the EA (stage 1\_EATA) and the ground have a low resistance value ( $1/gm4$  and  $1/gm5$ ); therefore, the power supply noise of stage 1\_EATA can be attenuated at nodes  $v_x$  and  $v_y$ . Only a small level of power supply noise can be coupled to nodes  $v_x$  and  $v_y$ , as they appear in the form of a common mode input ( $v_{icm}$  in Figure 3) to the output stage of the EA (stage 2\_EA). We first assume that the power noise is propagated by stage 1\_EATA through the common mode signal  $v_{icm}$  and causes a fluctuation on  $v_{g6}$ . The output  $v_g$  induced by  $v_{icm}$  is, therefore, given by

$$v_g = (gm7 v_{g6} - gm9 v_{icm}) \cdot (rO7 || rO9) \approx 0 \dots(3)$$

where we assume that  $M_{EA8}$  and  $M_{EA9}$  are matched devices ( $gm8 = gm9$ ), ( $rO8 \approx 1/gm6$ ), and ( $gm6 \approx gm7$ ). To cause  $gm6$  to be close to  $gm7$ , the channel length of  $M_{EA6}$  and  $M_{EA7}$  are selected to be five times the minimum length to reduce the effect of channel-length modulation. Then, we ground both the nodes  $v_x$  and  $v_y$  and input the power noise from the power supply ( $V_{DD}$ ). The small-signal model shown at the top of Figure 3 is used to show how the power noise is replicated to  $v_g$ .

Application of the superposition theorem by summing (3) and (4), we see that almost the entire power supply noise is replicated to the gate terminal of  $M_p(v_g)$ . As the frequency of the power noise increases, the small-signal model shown in Figure 3 is no longer valid as the equivalent impedance of the parasitic capacitance of  $M_p(C_{gs}/C_{gd})$  becomes finite and can no longer be ignored. As  $C_{gs}/C_{gd}$  equals 1.4/0.5 pF in our design, the PSR is expected to fall when the frequency of the power noise goes  $>100$  kHz. The first stage of the EA and  $M_{ta1} - M_{ta8}$  constitutes the TA that reduces the slew time of the gate terminal of  $M_p$  by increasing the dynamic discharging/charging current during the load transient. The first stage of the EA is reused as a part of the output variation detector of the TA to reduce the circuit complexity. Furthermore, to avoid a significant increase in  $I_Q$  and to avoid the breaking of perfect replication of the power noise at the gate terminal of  $M_p$ ,  $M_{ta3}$ , and  $M_{ta8}$  are biased at the cutoff region in the steady state. A large load change causes a variation in both the output voltage ( $v_{OUT}$ ) and feedback voltage ( $v_{FB}$ ).

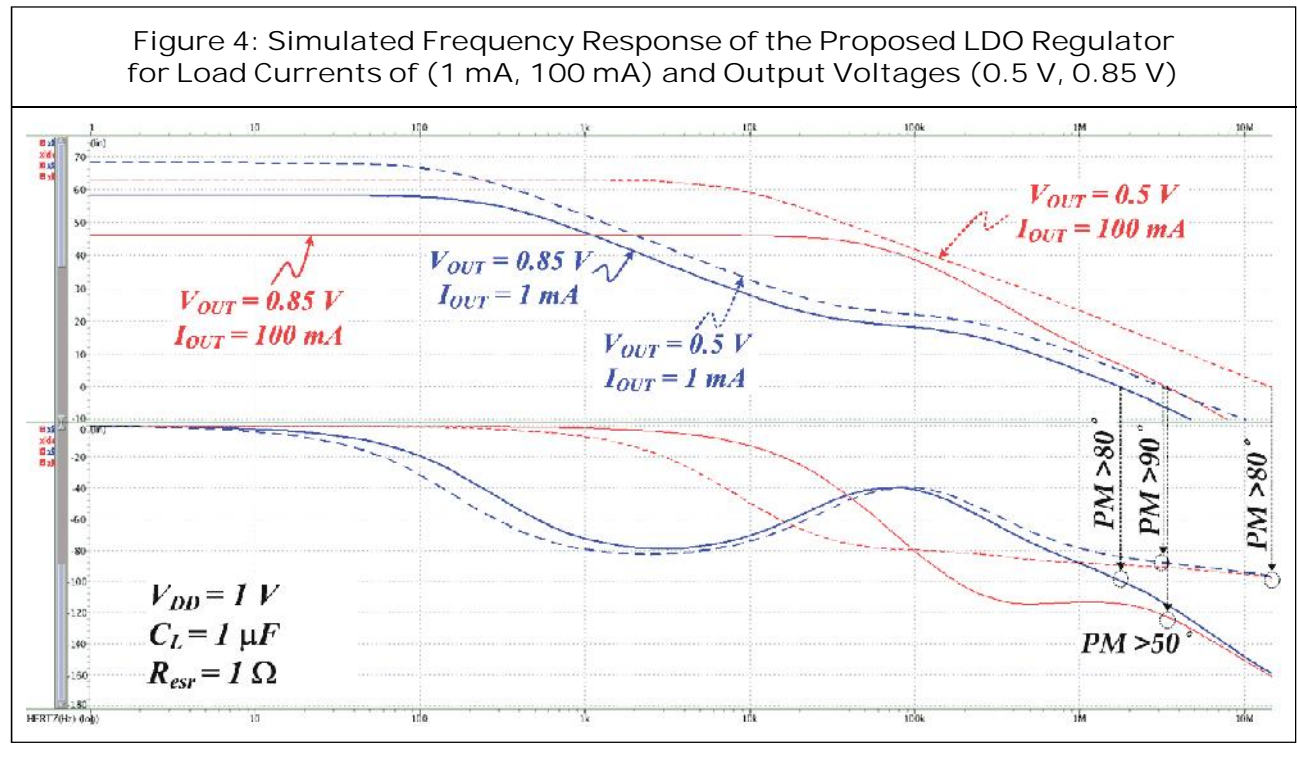
The proposed LDO regulator shown in Figure 2 has three poles ( $p_o$ ,  $p_x$ , and  $p_g$ ) and

one zero ( $z_{esr}$ ), and the simulated frequency response of the loop gain for different load currents ( $I_{OUT} = 1$  and  $100$  mA), output voltage ( $V_{OUT} = 0.5$  and  $0.85$  V) are shown in Figure 4. The dominant pole is  $p_o$  (100-10 kHz) due to the large off-chip compensation capacitor  $C_L$  (1 ~F). The second dominant pole ( $p_g$ ) is located at a relatively high frequency (~100 kHz) as the wide output swing of the EA reduces the size of the  $M_p$ . Thus,  $p_g$  can be easily cancelled by the zero ( $z_{esr}$ ). The third pole ( $p_x$ ) is far beyond the UGF because of the simple architecture of the OTA-based EA, and therefore does not affect the stability. Figure 4 guarantees the stability of the proposed LDO regulator for a wide range of operating conditions.

### EXPERIMENTAL RESULTS AND THE PERFORMANCE EVALUATIONS

The proposed LDO regulator is fabricated using a 90-nm CMOS process. The core area

is only  $0.0041$  mm<sup>2</sup> and the maximum load current is  $100$  mA. The input voltage is  $1$  V and the values of  $R_1$  and  $R_2$  can be adjusted to generate any regulated output level between  $0.85$  and  $0.5$  V. The maximum  $I_Q$  is  $60$  ~A, achieving a  $99.94\%$  current efficiency. The  $C_L$  used for measurement is  $1$  ~F with a  $R_{esr}$ . The input/output voltage  $V_{DD}$  and  $V_{OUT}$  is set to  $\{1$  V,  $0.85$  V $\}$  and  $\{1$  V,  $0.5$  V $\}$ , respectively. The output variations during load transient ( $\Delta V_{OUT}$ ) are measured to be only  $28$  and  $24$  mV for  $V_{OUT}$  equal to  $0.85$  and  $0.5$  V, respectively. The rise/fall time ( $10$  ~s) of the load current transient is restricted by the limitation of our measurement instrument (Chroma Electronic Load System 6300 Series). The ac capability of the proposed LDO regulator is, therefore, not tested to its best condition and the resulting small output variations are from enough dc loop gain. As the output variation of  $28$  mV is far less than the value of  $(100$  mA  $\times R_{esr})$ , we can, however,

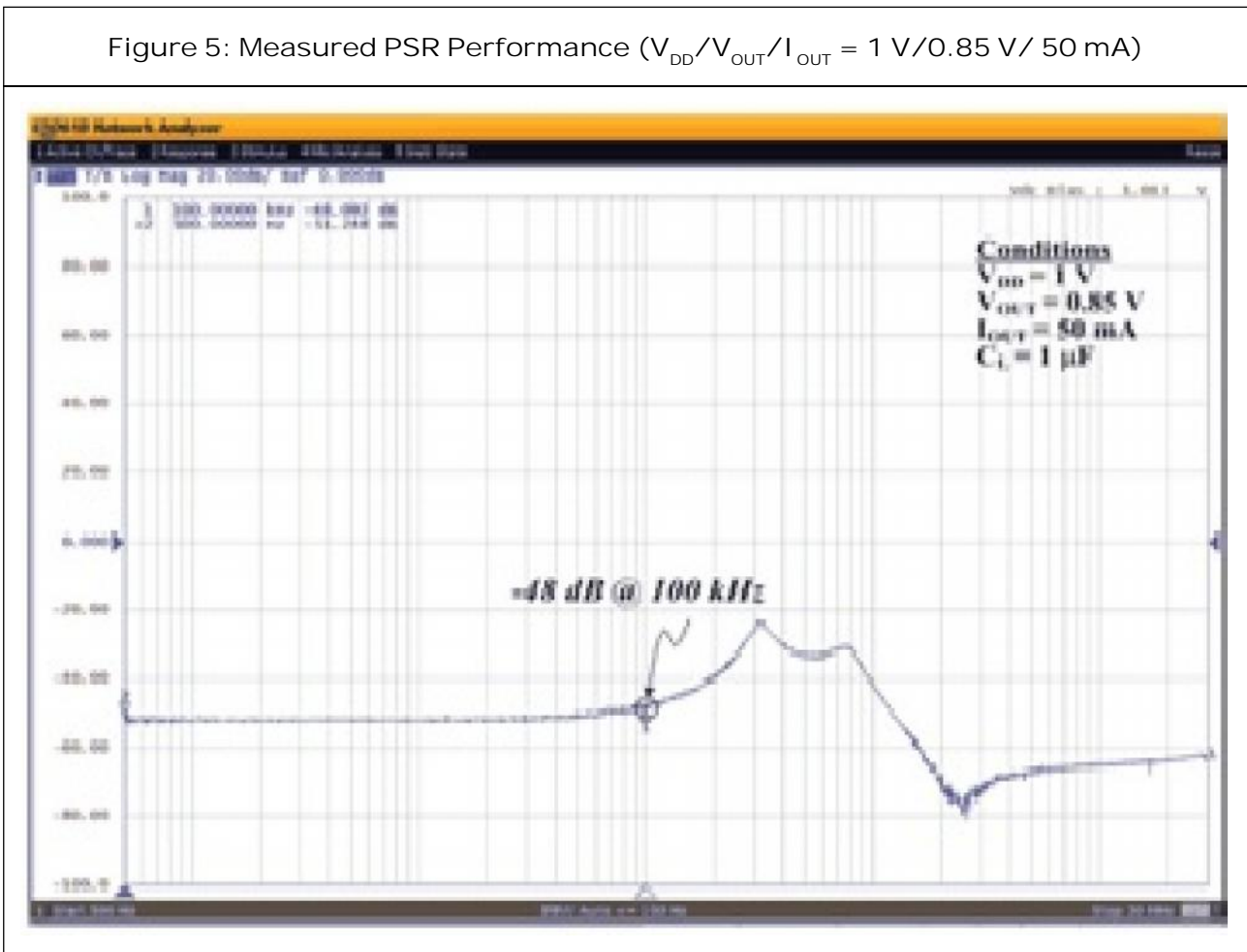


speculate that the response time of the LDO regulator test chip is far  $< 10^{-8}$  s. The PSR performance is also measured when the test conditions are  $V_{DD} = 1$  V,  $V_{OUT} = 0.85$  V, and  $I_{OUT} = 50$  mA; the measured result is shown in Figure 5. The proposed LDO regulator achieves a PSR  $\sim 50$  dB at low frequencies whereas the rolloff frequency is  $\sim 100$  kHz. Although the consumed  $I_Q$  is larger than the design in [6], the proposed LDO regulator benefits from superior performance in output variations. In contrast, Lam and Ki (2008) produced the smallest output variation (0-50 mA), yet consumed a significant  $I_Q$ . To fairly evaluate the performance of the load transient response, the frequently used figure of merit

(FOM1) proposed in Hazucha *et al.* (2005) was adopted to include the dependence of the output capacitance. The design in Garimella *et al.* (2010) had a better FOM1 than the proposed design; however, it did not show the dominant ESR effects of output variation during the load transient. Further, Garimella *et al.* (2010) was unable to operate below 1-V input voltage, and does not report the PSR performance. We also use FOM2 that is  $(FOM1 \times \text{area})$  to show the area efficiency further.

In summary, the proposed LDO regulator is compact in size, and achieves a high PSR, fast transient response, and high current efficiency for low-voltage operation.

Figure 5: Measured PSR Performance ( $V_{DD}/V_{OUT}/I_{OUT} = 1$  V/0.85 V/ 50 mA)



## CONCLUSION

This paper presented an LDO regulator using a simple OTA-type EA plus an adaptive transient accelerator, which can achieve operation below 1 V, fast transient response, low  $I_Q$ , and high PSR under a wide range of operating conditions. The proposed LDO regulator was designed and fabricated using a 90-nm CMOS process to convert an input of 1 V to an output of 0.85-0.5 V, while achieving a PSR of ~50 dB with a 0-100-kHz frequency range. In addition, a 28-mV maximum output variation for a 0-100-mA load transient, and a 99.94% current efficiency was achieved. The experimental results verified the feasibility of the proposed LDO regulator. 🌟

## ACKNOWLEDGMENT

The authors would like to thank the National Chip Implementation Center of Taiwan for the chip fabrication service. The authors would also like to thank W-J Chen for his assistances during chip measurement.

## REFERENCES

1. Al-Shyoukh M, Lee H and Perez R (2007), "A Transient-Enhanced Low-Quiescent Current Low-Dropout Regulator with Buffer Impedance Attenuation", *IEEE J. Solid-State Circuits*, Vol. 42, No. 8, pp. 1732-1742.
2. Chen C, Wu J H and Wang Z X (2011), "150 mA LDO with Self-Adjusting Frequency Compensation Scheme", *Electron. Lett.*, Vol. 47, No. 13, pp. 767-768.
3. El-Nozahi M, Amer A, Torres J, Entesari K and Sanchez-Sinencio E (2010), "High PSR Low Drop-Out Regulator with Feed-Forward Ripple Cancellation Technique", *IEEE J. Solid-State Circuits*, Vol. 45, No. 3, pp. 565-577.
4. Garimella A, Rashid M W and Furth P M (2010), "Reverse Nested Miller Compensation Using Current Buffers in a Three-Stage LDO", *IEEE Trans. Circuits Syst. II, Exp. Briefs*, Vol. 57, No. 4, pp. 250-254.
5. Hazucha P, Karnik T, Bloechel B A, Parsons C, Finan D and Borkar S (2005), "Area-Efficient Linear Regulator with Ultra-Fast Load Regulation", *IEEE J. Solid-State Circuits*, Vol. 40, No. 4, pp. 993-940.
6. Hu J, Hu B, Fan Y and Ismail M (2011), "A 500 nA Quiescent, 100 mA Maximum Load CMOS Low-Dropout Regulator", in Proc. IEEE Int. Conf. Electron. Circuits Syst., December, pp. 386-389.
7. Lam Y-H and Ki W-H (2008), "A 0.9 V 0.35  $\mu$ m Adaptively Biased CMOS LDO Regulator with Fast Transient Response", in Proc. IEEE Int. Solid-State Circuits Conf., February, pp. 442-443 & 626.
8. Lee Y-H, Yang Y-Y, Chen K-H, Lin Y-H, Wang S-J, Zheng K-L, Chen P-F, Hsieh C-Y, Ke Y-Z, Chen Y-K and Huang C-C (2010), "A DVS Embedded System Power Management for High Efficiency Integrated SoC in UWB System", *IEEE J. Solid-State Circuits*, Vol. 45, No. 11, pp. 2227-2238.
9. Lin H-C, Wu H-H and Chang T-Y (2008), "An Active-Frequency Compensation Scheme for CMOS Low-Dropout Regulators with Transient-Response Improvement", *IEEE Trans. Circuits Syst. II, Exp. Briefs*, Vol. 55, No. 9, pp. 853-857.

10. Patel A P and Rincon-Mora G A (2010), "High Power-Supply-Rejection (PSR) Current-Mode Low-Dropout (LDO) Regulator", *IEEE Trans. Circuits Syst. II, Exp. Briefs*, Vol. 57, No. 11, pp. 868-873.
11. Rincon-Mora G A (2009), *Analog IC Design with Low-Dropout Regulators*, Ch. 1, McGraw-Hill, New York, USA.
12. Sansen W M C (2008), *Analog Design Essentials*, Ch. 7, Springer-Verlag, New York, USA.
13. Zhan C and Ki W-H (2011), "An Adaptively Biased Low-Dropout Regulator with Transient Enhancement", in Proc. Asia South Pacific Design Autom. Conf., pp. 117-118.